

## STRUCTURAL AND LUMINESCENCE PROPERTIES OF $Pb^{2+}$ DOPED $Li_6Gd(BO_3)_3$ PHOSPHOR

E. Erdoğan<sup>1\*</sup>, E. Yıldız<sup>2</sup>

<sup>1</sup> Bartın University, Department of Environmental Engineering, 74100 Bartın, Turkey; e-mail: eerdogmus@bartin.edu.tr

<sup>2</sup> Yozgat Bozok University, Department of Chemistry, 66900 Yozgat, Turkey

We synthesized pure and  $Pb^{2+}$  ion doped  $Li_6Gd(BO_3)_3$  phosphors via the solid-state reaction method at 700°C for 5 h in air. The phase analysis of the synthesized materials was determined using DTA/TGA, XRD, and FTIR. The photoluminescence characteristics of pure and  $Pb^{2+}$  doped phosphors were investigated at room temperature using a photoluminescence spectrophotometer. The emission and excitation bands of  $Pb^{2+}$  doped  $Li_6Gd(BO_3)_3$  were observed at 313 and 242 nm, respectively. The dependence of the PL intensities on the  $Pb^{2+}$  concentration for the  $Li_6Gd_{1-x}Pb_x(BO_3)_3$  ( $0.005 \leq x \leq 0.025$ ) phosphors was also studied. The highest emission intensity was obtained from 0.02 mol  $Pb^{2+}$  doped  $Li_6Gd(BO_3)_3$ .

**Keywords:** phosphor, photoluminescence,  $Li_6Gd(BO_3)_3$ ,  $Pb^{2+}$ .

## СТРУКТУРНЫЕ И ЛЮМИНЕСЦЕНТНЫЕ СВОЙСТВА ЛЮМИНОФОРА $Li_6Gd(BO_3)_3$ , ЛЕГИРОВАННОГО ИОНАМИ $Pb^{2+}$

E. Erdoğan<sup>1\*</sup>, E. Yıldız<sup>2</sup>

УДК 535.37

<sup>1</sup> Бартынский университет, 74100 Бартын, Турция; e-mail: eerdogmus@bartin.edu.tr

<sup>2</sup> Университет Йозгат Бозок, 66900 Йозгат, Турция

(Поступила 20 марта 2019)

Методом твердофазной реакции при 700 °С в течение 5 ч на воздухе синтезированы чистые и легированные ионами  $Pb^{2+}$  люминофоры  $Li_6Gd(BO_3)_3$ . Фазовый состав синтезированных материалов определен с помощью методов DTA/TGA, XRD и FTIR. Фотолюминесцентные характеристики чистых и легированных  $Pb^{2+}$  люминофоров исследованы при комнатной температуре с помощью фотолюминесцентного спектрофотометра. Полосы излучения и возбуждения легированного  $Pb^{2+}$   $Li_6Gd(BO_3)_3$  наблюдались при 313 и 242 нм. Исследована зависимость интенсивностей фотолюминесценции от концентрации  $Pb^{2+}$  для люминофоров  $Li_6Gd_{1-x}Pb_x(BO_3)_3$  ( $0.005 \leq x \leq 0.025$ ). Наибольшая интенсивность излучения получена от 0.02 моль  $Li_6Gd(BO_3)_3$ , легированного  $Pb^{2+}$ .

**Ключевые слова:** люминофор, фотолюминесценция,  $Li_6Gd(BO_3)_3$ ,  $Pb^{2+}$ .

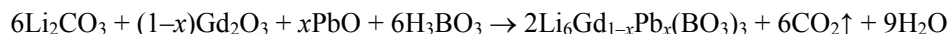
**Introduction.** In recent years, the study of borate crystals and glasses has attracted considerable interest due to their attractive optical and physical properties and wide practical applications. In particular, borate compounds, undoped and doped with rare-earth and transition elements, are promising materials for nonlinear optics, quantum electronics, and laser technology [1–6], scintillators and thermoluminescence dosimeters [7–11], detectors and transformers of ionizing radiation [12, 13] and many other applications [14–16]. From the technological point of view, glassy borate compounds are more promising materials than their crystalline analogues. The growth technology of the borate single crystals is a difficult, long-term, and very expensive process, whereas large high-quality samples of borate glasses can be obtained in a simple, fast, and inexpensive way [17].

The  $\text{Pb}^{2+}$  ion, as a well-known dopant for many different matrices, is of great scientific and technological interest. Due to the diversity of its luminescent properties, it provides the possibilities of fabricating novel luminescent materials. Usually, the luminescence of the  $\text{Pb}^{2+}$  ion ( $6s^2$ ) is characterized by the ground state  $^1S_0$  and two excited states of singlet  $^1P_1$  and triplet  $^3P_{0,1,2}$  transitions, which originate from the  $6s^2-6s^16p^1$  inter-configurational transition [18–20]. It has been shown that the effect of the  $s^2$  ions on the ground state considerably complicates the situation (e.g., Jahn–Teller effect) [18]. Furthermore, the interaction of  $\text{Pb}^{2+}$  ions with the host lattice strongly influences its luminescent properties [21, 22].

Double orthoborate  $\text{Li}_6\text{RE}(\text{BO}_3)_3$  ( $R$  = trivalent rare earth ions) crystals are attractive matrix materials owing to their high transparency in the UV and high damage threshold upon exposure to energetic radiations [23]. When activated with RE ions, these materials can also be used as scintillation detectors for thermal neutrons and gamma photons.  $\text{Li}_6\text{RE}(\text{BO}_3)_3$  compounds are known to crystallize in the monoclinic system with space group  $\text{P}2_1/c$  and have an isostructural nature, as a result of which the host lattice can be isomorphically substituted [24]. Recently, the luminescence properties of  $\text{Ce}^{3+}$  [25–27],  $\text{Tb}^{3+}$  [28],  $\text{Eu}^{3+}$  [29, 30], and  $\text{Tm}^{3+}$  [31] doped  $\text{Li}_6\text{Gd}(\text{BO}_3)_3$  have been intensively studied. However, until now there has been no research of the luminescence properties of the  $\text{Pb}^{2+}$  doped  $\text{Li}_6\text{Gd}(\text{BO}_3)_3$  compound.

In this study, pure and  $\text{Li}_6\text{Gd}(\text{BO}_3)_3$  phosphors with different mole ratios of  $\text{Pb}^{2+}$  were prepared by the solid state reaction method. The synthesized materials were characterized using DTA/TGA, XRD, and FTIR. After synthesis and characterization of the phosphors, the photoluminescence properties were studied using a photoluminescence spectrophotometer at room temperature.

**Experimental.** Pure and  $\text{Li}_6\text{Gd}_{1-x}\text{Pb}_x(\text{BO}_3)_3$  ( $x = 0.005, 0.01, 0.015, 0.020, \text{ and } 0.025$ ) powders were synthesized using the solid-state reaction method at  $700^\circ\text{C}$  for 5 h in air. As starting materials,  $\text{Li}_2\text{CO}_3$  (Sigma-Aldrich  $\geq 99\%$ ),  $\text{H}_3\text{BO}_3$  (Merck  $\geq 99.8\%$ ),  $\text{PbO}$  (Merck  $\geq 99.8\%$ ), and  $\text{Gd}_2\text{O}_3$  (Sigma-Aldrich  $\geq 99\%$ ) reactants were used. The raw materials were weighed in proportions according to the following chemical reaction:



Initially, stoichiometric amounts of the starting reagents were thoroughly mixed and ground together in an agate mortar and placed in an alumina crucible. Later, the powder materials in the alumina crucible were pre-sintered in a muffle furnace at about  $450^\circ\text{C}$  for 2 h in air. The preheated treated powders were removed from the muffle furnace and re-milled. Then the obtained powders well thoroughly mixed and slowly heated at  $700^\circ\text{C}$  for 5 h in air.

The crystal structure of the pure and  $\text{Pb}^{2+}$  doped  $\text{Li}_6\text{Gd}(\text{BO}_3)_3$  powders was determined on an X-ray Phillips X'Pert Pro equipped with  $\text{CuK}\alpha$  (30 kV, 15 mA,  $1.54051 \text{ \AA}$ ) radiation at room temperature. The Fourier infrared spectra between  $500$  and  $3500 \text{ cm}^{-1}$  was measured at room temperature with a Shimadzu 8303 FTIR spectrometer. A DTA/TG combined system (Perkin Elmer Diamond, USA) was used to determine the reaction conditions in the temperature range of  $100$ – $1000^\circ\text{C}$  under an inert  $\text{N}_2$  atmosphere with a heating rate of  $10^\circ\text{C}/\text{min}$ . The photoluminescence characteristics of undoped and  $\text{Pb}^{2+}$  doped phosphors were investigated using a Scinco FluoroMate FS-2 spectrofluorometer equipped with a 150W Xe-arc lamp at room temperature.

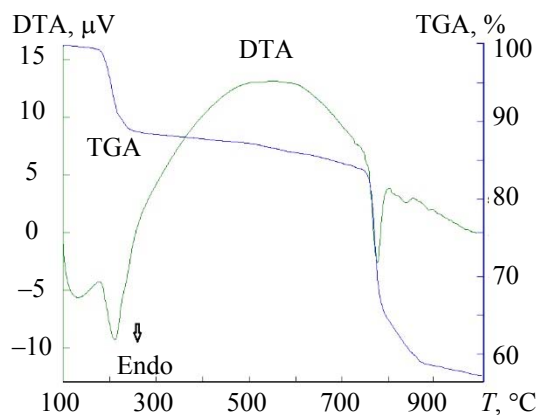


Fig. 1. DTA/TGA curves of the precursor.

**Results and discussion.** *Thermogravimetry (DTA/TGA) analysis.* The thermal decomposition of the prepared powder was analyzed by simultaneous thermogravimetric analysis (TGA) and differential thermal

analysis (DTA) in the temperature range from 100 to 1000°C in air with a heating rate of 10°C/min. The DTA/TGA curves of the precursor are given in Fig. 1. The thermograms showed a small endothermic peak corresponding to the melting of H<sub>3</sub>BO<sub>3</sub> near 135°C. Subsequently, another strong endothermic peak appeared at 210°C, which indicated the dissociation of H<sub>3</sub>BO<sub>3</sub> to B<sub>2</sub>O<sub>3</sub> and H<sub>2</sub>O. This was confirmed from the DTA of boric acid and the thermodynamic data. The weight of the sample decreased drastically just after the dissociation of boric acid. The thermograms revealed an endothermic peak at 780°C due to the melting of Li<sub>6</sub>Gd(BO<sub>3</sub>)<sub>3</sub>. This means that the decomposition is almost complete and the crystallization of the Li<sub>6</sub>Gd(BO<sub>3</sub>)<sub>3</sub> occurs at 700°C.

*X-ray powder diffraction analysis.* Figure 2 illustrates the XRD pattern of the pure and Pb<sup>2+</sup> ion doped (0.005, 0.01, 0.015, 0.02, and 0.025 mol) powders after heating at 700°C. All the strong reflection peaks of the patterns can be indexed as pure monoclinic symmetry, space group *P2<sub>1</sub>/c*, with crystal lattice parameters  $a = 7.2277 \text{ \AA}$ ,  $b = 16.5057 \text{ \AA}$ ,  $c = 6.6933 \text{ \AA}$ ,  $\beta = 105.3737^\circ$ , which are in a good agreement with the literature (JCPDS Card Number 54-1119) [24].

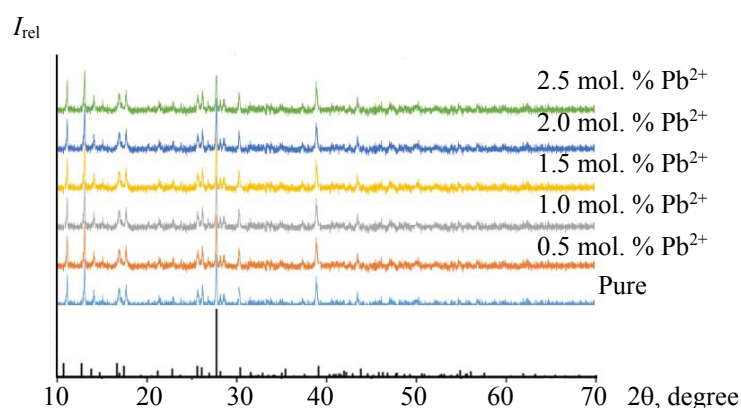


Fig. 2. XRD patterns of Li<sub>6</sub>Gd(BO<sub>3</sub>)<sub>3</sub> and Li<sub>6</sub>Gd<sub>1-x</sub>Pb<sub>x</sub>(BO<sub>3</sub>)<sub>3</sub> ( $x = 0.005, 0.01, 0.015, 0.02, \text{ and } 0.025$ ) phosphors and the standard data JCPDS card No. 54-1119 of Li<sub>6</sub>Gd(BO<sub>3</sub>)<sub>3</sub> compound.

It is seen from the results that Pb<sup>2+</sup> ions implanted into the Li<sub>6</sub>Gd(BO<sub>3</sub>)<sub>3</sub> compound do not change the lattice structure of the sample. This indicated that Pb<sup>2+</sup> could be doped into the Li<sub>6</sub>Gd(BO<sub>3</sub>)<sub>3</sub> material instead of Gd<sup>3+</sup> up to a mole fraction of 0.025 without any additional phase formation.

*Infrared spectrum analysis.* The infrared spectrum of the Li<sub>6</sub>Gd(BO<sub>3</sub>)<sub>3</sub> is presented in Fig. 3. As usual, the frequencies of B–O vibrations depend on the boron coordination. IR spectra of Li<sub>6</sub>Gd(BO<sub>3</sub>)<sub>3</sub> were measured at room temperature. The stretching frequencies of a coordinated BO<sub>*n*</sub> groups decrease as the coordination number *n* increases. The IR absorption at wavenumbers smaller than 500 cm<sup>-1</sup> originates mainly from the lattice dynamic modes. The Li<sub>6</sub>Gd(BO<sub>3</sub>)<sub>3</sub> material from the analysis of the spectrum IR, BO<sub>3</sub><sup>3-</sup> ion has been identified as two triangular BO<sub>3</sub> groups at one corner sharing an O atom. The boron coordination is the deciding factor of B–O frequencies. For an isolated, triangular BO<sub>3</sub> group, the vibrations are in the region  $\nu_3 = 1100\text{--}1500 \text{ cm}^{-1}$  (asymmetric stretch of B–O),  $\nu_1 = 900\text{--}1000 \text{ cm}^{-1}$  (symmetric stretch of B–O),  $\nu_2 = 700\text{--}900 \text{ cm}^{-1}$  (out-of-plane bend), and  $\nu_4 = 450\text{--}650 \text{ cm}^{-1}$  (in-plane bend) [32, 33].

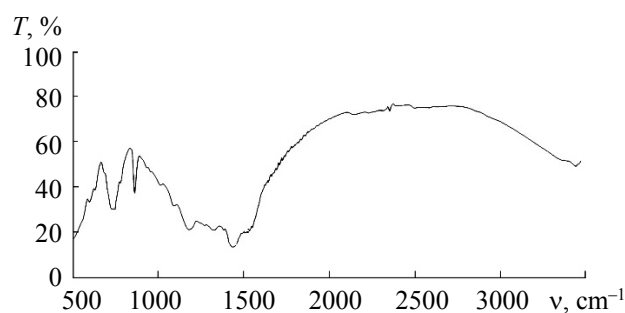


Fig. 3. The infrared spectrum of Li<sub>6</sub>Gd(BO<sub>3</sub>)<sub>3</sub> at room temperature.

*Photoluminescence properties of  $\text{Li}_6\text{Gd}(\text{BO}_3)_3:\text{Pb}^{2+}$  phosphor.* The ground state of the free ion is  $^1S_0$ , while the  $6s^2-6s^16p^1$  excited states give rise to triplet levels ( $^3P_0, ^3P_1, ^3P_2$ ) and the  $^1P_1$  singlet state. The lowest energy  $^1S_0 \rightarrow ^3P_0$  transition is strongly forbidden, but the  $^1S_0 \rightarrow ^3P_1$  transition and the  $^1S_0 \rightarrow ^3P_2$  transition become allowed due to spin-orbit coupling and coupling to asymmetrical phonon modes, respectively. The  $^1S_0 \rightarrow ^1P_1$  transition is an allowed electric dipole transition [34, 35]. Figure 4 shows the excitation and emission spectra of the undoped- $\text{Li}_6\text{Gd}(\text{BO}_3)_3$  and  $\text{Li}_6\text{Gd}(\text{BO}_3)_3:2\% \text{Pb}^{2+}$  phosphor. The PL properties can be obtained from the undoped sample. It is clear that introduction of the  $\text{Pb}^{2+}$  ion into  $\text{Li}_6\text{Gd}(\text{BO}_3)_3$  greatly changed the PL properties of  $\text{Li}_6\text{Gd}(\text{BO}_3)_3$ . Thus,  $\text{Pb}^{2+}$ -doped  $\text{Li}_6\text{Gd}(\text{BO}_3)_3$  is representative of a new class of luminescent material.

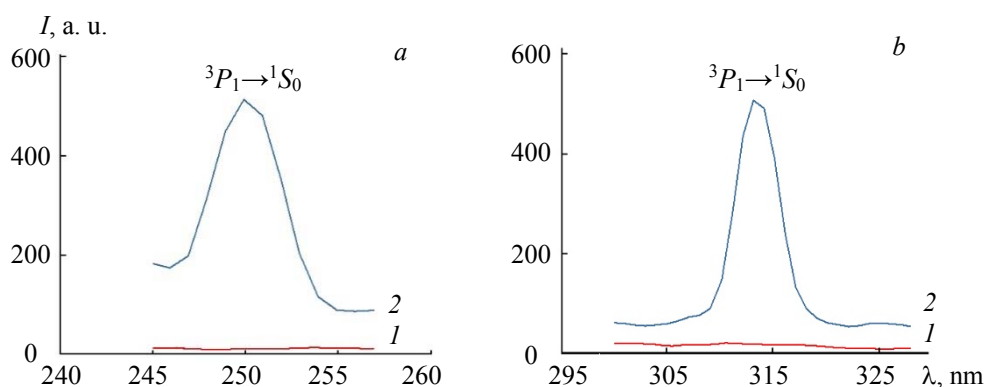


Fig. 4. Excitation (a), and emission (b) spectra of (1) undoped- $\text{Li}_6\text{Gd}(\text{BO}_3)_3$ , and (2)  $\text{Li}_6\text{Gd}_{1-x}\text{Pb}_x(\text{BO}_3)_3$  ( $x = 0.02$ ) at room temperature.

As can be seen from Fig. 4a, the excitation spectrum of the samples shows a broad band centered near 242 nm, which is assigned to the  $^1S_0 \rightarrow ^3P_1$  transition. The emission band was observed at 313 nm from the  $^3P_1$  excited state level to the  $^1S_0$  ground state (Fig. 4b). Additionally, we observed no splitting or multiple bands in the emission spectra for prepared phosphors; therefore, we believe that the  $\text{Pb}^{2+}$  ions are incorporated into only one site ( $\text{Gd}^{3+}$  sites and not  $\text{Li}^+$  sites) in the crystal lattice. The luminescence behavior of  $\text{Pb}^{2+}$  in  $\text{Li}_6\text{Gd}(\text{BO}_3)_3$  is sensitive to the covalence of  $\text{Pb}^{2+}-\text{O}^{2-}$  bonds. On the other hand, the energy of the activator ions ( $\text{Pb}^{2+}$ ) is closely related to the degree of covalence of the activator ion ( $\text{Pb}^{2+}$ )-ligand ( $\text{O}^{2-}$ ) bonds [36]. In many inorganic hosts, the emission band of  $\text{Pb}^{2+}$  ion is in the UV region. It is also known that in some hosts,  $\text{Pb}^{2+}$  ion emits in the visible region. This diversity is strongly dependent on the site occupied by  $\text{Pb}^{2+}$  ions, electronegativity of the ligand, crystal structure of the host lattice, and temperature [37].

*Change of photoluminescence properties of  $\text{Li}_6\text{Gd}(\text{BO}_3)_3$  depending on the  $\text{Pb}^{2+}$  ion concentration.* It is known that the PL intensities of  $\text{Pb}^{2+}$  doped inorganic phosphors always depend on the doped  $\text{Pb}^{2+}$  ion concentration. So, the emission spectra of the  $\text{Pb}^{2+}$  doped  $\text{Li}_6\text{Gd}(\text{BO}_3)_3$  samples with different  $\text{Pb}^{2+}$  doping concentrations were investigated at room temperature. The dependence of the emission intensity on the  $\text{Pb}^{2+}$  concentration for undoped  $\text{Li}_6\text{Gd}(\text{BO}_3)_3$  and  $\text{Li}_6\text{Gd}_{1-x}\text{Pb}_x(\text{BO}_3)_3$  ( $x = 0.005, 0.01, 0.015, 0.02$ , and  $0.025$ ) is shown in Fig. 5a ( $\lambda_{\text{ex}} = 242$  nm).

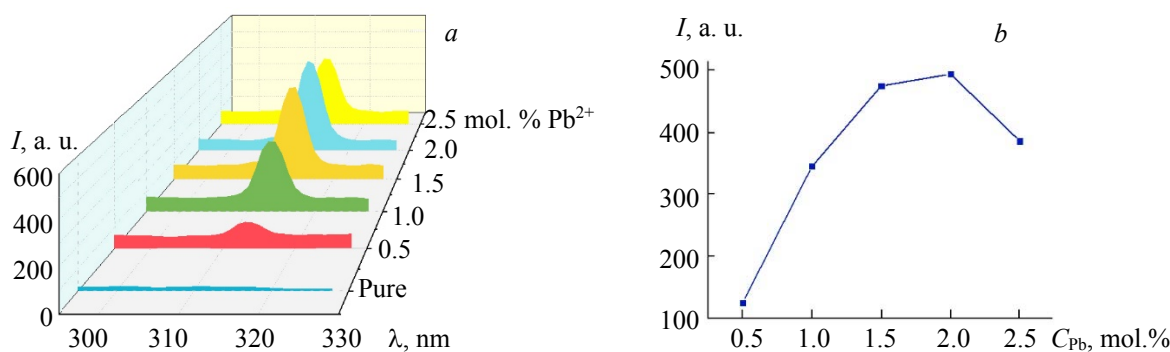


Fig. 5. Photoluminescence spectra (a), and relative photoluminescence intensity (b) of pure and  $\text{Li}_6\text{Gd}_{1-x}\text{Pb}_x(\text{BO}_3)_3:\text{Pb}^{2+}$  ( $x = 0.005, 0.01, 0.015, 0.02$ , and  $0.025$  mole;  $\lambda_{\text{ex}} = 242$  nm).

As can be seen from Fig. 5b, with increasing Pb<sup>2+</sup> concentration, the emission intensity of Li<sub>6</sub>Gd(BO<sub>3</sub>)<sub>3</sub> increases and reaches a maximum at 0.02 mole. However, when the mol concentration of the Pb<sup>2+</sup> ion exceeds this concentration level, the emission intensity dramatically decreases due to the concentration quenching. The concentration quenching in inorganic phosphors has been attributed to the migration of excitation energy to the quenching centers (traps) or to the cross-relaxation mechanisms. At low Pb<sup>2+</sup> ion concentrations, the luminescence centers are separated, and only a small amount of energy transfers to the traps. When the Pb<sup>2+</sup> ion concentration in the host exceeds 0.02 mol, the energy can be easily transferred from one luminescence center to another, and the nonradiative combination processes increases gradually [38–42].

The Stokes shift of Pb<sup>2+</sup> doped Li<sub>6</sub>Gd(BO<sub>3</sub>)<sub>3</sub> compounds was calculated as 8051 cm<sup>-1</sup> using the excitation band at 242 nm and the emission band at 314 nm. Numerous articles have been published on the luminescence of Pb<sup>2+</sup> (6s<sup>2</sup>) in several host lattices. It is shown that the interaction of Pb<sup>2+</sup> with the host lattice strongly influences the value of the Stokes shift of the emission from the <sup>3</sup>P<sub>1</sub> excited state of Pb<sup>2+</sup> (see Table 1). So, there exists a relationship between the structure of the host and the magnitude of the Stokes shift. If we compare the Stokes shift of the Pb<sup>2+</sup> doped host lattices, the value of the Stokes shift of Li<sub>6</sub>Gd(BO<sub>3</sub>)<sub>3</sub>:Pb<sup>2+</sup> is small. The small Stokes shift of Li<sub>6</sub>Gd(BO<sub>3</sub>)<sub>3</sub>:Pb<sup>2+</sup> indicates a small relaxation in the excited state.

TABLE 1. Spectroscopic Properties of Some Pb<sup>2+</sup> Doped Inorganic Hosts at Room Temperature

Host	$\lambda_{\text{ex}}$ , nm	$\lambda_{\text{em}}$ , nm	Stokes shift, cm <sup>-1</sup>	Reference
LiCaBO <sub>3</sub>	265	296	3952	[19]
SrAl <sub>2</sub> B <sub>2</sub> O <sub>7</sub>	277	420	12292	[36]
Li <sub>2</sub> SrSiO <sub>4</sub>	271	381	10653	[43]
La <sub>2</sub> Sr <sub>5</sub> Mg(BO <sub>3</sub> ) <sub>6</sub>	254	361	9162	[44]
Sr <sub>6</sub> YAl(BO <sub>3</sub> ) <sub>6</sub>	277	371	9147	[44]
CaZr(BO <sub>3</sub> ) <sub>2</sub>	250	415	16000	[45]
Li <sub>6</sub> Gd(BO <sub>3</sub> ) <sub>3</sub>	250	313	8051	This study

**Conclusions.** In summary, we have successfully synthesized Li<sub>6</sub>Gd(BO<sub>3</sub>)<sub>3</sub>:Pb<sup>2+</sup> phosphors using the solid-state reaction method and characterized the obtained materials using DTA/TGA, XRD, FTIR, and PL spectra. The emission band of Li<sub>6</sub>Gd(BO<sub>3</sub>)<sub>3</sub>:Pb<sup>2+</sup> was observed at 313 nm from the <sup>3</sup>P<sub>1</sub> excited state level to the <sup>1</sup>S<sub>0</sub> ground state upon excitation with 242 nm. The dependence of the emission intensity on the Pb<sup>2+</sup> concentration for Li<sub>6</sub>Gd(BO<sub>3</sub>)<sub>3</sub> was studied in detail. It was observed that the concentration quenching of Pb<sup>2+</sup> in the host material is 0.02 mole. The Stokes shift for the prepared phosphor was calculated to be 8051 cm<sup>-1</sup>. Consequently, these materials are promising for UV-lamp phosphors.

## REFERENCES

1. R. Arun Kumar, *J. Chem.*, **1** (2013); doi 10.1155/2013/154862.
2. D. Xue, K. Betzler, H. Hesse, D. Lammers, *Solid State Commun.*, **114**, 21–25 (2000).
3. T. Sasaki, Y. Mori, M. Yoshimura, Y. K. Yap, T. Kamimura, *Mater. Sci. Eng. Rep.*, **30**, 1–54 (2000).
4. V. T. Adamiv, Ya. V. Burak, I. M. Teslyuk, *J. Cryst. Growth*, **289**, 157–160 (2006).
5. B. V. Padlyak, V. T. Adamiv, Ya. V. Burak, M. Kolcun, *Physica B*, **412**, 79–82 (2013).
6. G. E. Malashkevich, V. N. Sigaev, N. V. Golubev, E. Kh. Mamadzhanova, A. V. Danil'chik, V. Z. Zubelevich, E. V. Lutsenko, *JETP Lett.*, **92**, 497–501 (2010).
7. M. Prokic, *Radiat. Meas.*, **33**, 393–396 (2001).
8. M. F. Dubovik, T. I. Korshikova, Yu. S. Oseledchik, S. V. Parkhomenko, A. L. Prosvirnin, N. V. Svitanko, A. V. Tolmachev, R. P. Yavetsky, *Funct. Mater.*, **12**, 685–688 (2005).
9. A. C. Fernandes, M. Osvay, J. P. Santos, V. Holovey, M. Ignatovych, *Radiat. Meas.*, **43**, 476–479 (2008).
10. I. N. Ogorodnikov, N. E. Poryvai, *J. Lumin.*, **132**, 1318–1324 (2012).
11. A. Un, *Radiat. Phys. Chem.*, **85**, 23–25 (2013).
12. M. Ishii, Y. Kuwano, S. Asaba, T. Asai, M. Kawamura, N. Senguttuvan, T. Hayashi, M. Koboyashi, M. Nikl, S. Hosoya, K. Sakai, T. Adachi, T. Oku, H. M. Shimizu, *Radiat. Meas.*, **38**, 571–574 (2004).
13. B. I. Zadneprowski, N. V. Eremin, A. A. Paskhalov, *Funct. Mater.*, **12**, 261–267 (2005).
14. E. W. Deeg, In: *Industrial Borate Glasses*, Eds. L. D. Pye, V. D. Frechette, N. J. Kreidl, Plenum Press, New York, 587–596 (1978).

15. D. Ehrt, *Glass Technol.*, **41**, 182–185 (2000).
16. R. Komatsu, H. Kawano, Z. Oumarou, K. Shinoda, V. Petrov, *J. Cryst. Growth*, **275**, 843–847 (2005).
17. B. V. Padlyak, S. I. Mudry, Y. O. Kulyk, A. Drzewiecki, V. T. Adamiv, Y. V. Burak, I. M. Teslyuk, *Mater. Sci. Pol.*, **30**, 264–273 (2012).
18. Q. Wang, Z. Mu, S. Zhang, X. Feng, Q. Zhang, D. Zhu, Y. Yang, F. Wu, *Optik*, **174**, 56–61 (2018).
19. I. Pekgozlu, E. Erdogmus, S. Cubuk, A. S. Basak, *J. Lumin.*, **132**, 1394–1399 (2012).
20. G. Blasse, *Prog. Solid-State Chem.*, **18**, 79–171 (1998).
21. J. Chaminade, V. Jubera, A. Garcia, P. Gravereau, C. Fouassier, *J. Optoelectron. Adv. Mater.*, **2**, 451–458 (2000).
22. S. P. Bhagat, A. B. Gawande, S. K. Omanwar, *Opt. Mater.*, **40**, 36–40 (2015).
23. J. Sablayrolles, V. Jubera, J.-P. Chaminade, I. Manek-Höninger, S. Murugan, T. Cardinal, R. Olazcuaga, A. Garcia, F. Salin, *Opt. Mater.*, **27**, 1681–1685 (2005).
24. É. Tichy-Rács, Á. Péter, V. Horváth, K. Polgár, K. Lengyel, L. Kovács, *Mater. Sci. Forum.*, **729**, 493–496 (2013).
25. S. Pana, J. Zhanga, J. Pana, G. Ren, N. Lic, Z. Wuc, Y. Heng, *J. Alloys Compd.*, **751**, 129–137 (2018).
26. I. N. Ogorodnikov, V. A. Pustovarov, *J. Lumin.*, **134**, 113–125 (2013).
27. V. N. Baumer, M. F. Dubovik, B. V. Grinyov, T. I. Korshikova, A. V. Tolmachev, A. N. Shekhovtsov, *Radiat. Meas.*, **38**, 359–362 (2004).
28. F. Zhanga, Y. Wanga, Y. Taob, *Phys. Procedia*, **29**, 55–61 (2012).
29. P. Chen, F. Mo, A. Guan, R. Wang, G. Wang, S. Xia, L. Zhou, *Appl. Radiat. Isotop.*, **108**, 148–153 (2016).
30. M. M. Yawalkar, G. D. Zade, V. Singh, S. J. Dhoble, *J. Mater. Sci: Mater. Electron.*, **28**, 180–189 (2017).
31. X. Ma, J. Li, Z. Zhu, Z. You, Y. Wang, C. Tu, *J. Lumin.*, **128**, 1660–1664 (2008).
32. W. G. Zou, M. K. Lü, F. Gu, S. Wang, Z. Xiu, G. Zhou, *Mater. Sci. Eng. B*, **127**, 134–137 (2006).
33. G. Blasse, *Solid State Chem.*, **18**, 79–171 (1998).
34. A. A. Setlur, A. M. Srivastava, *Opt Mater.*, **29**, 410–415 (2006).
35. M. Paraschiva, I. Nicoara, M. Steff, M. Bunoiu, *Acta Phys. Pol. A*, **117**, 466–470 (2010).
36. I. Pekgözlü, S. Taşcıoğlu, A. Menger, *Inorg. Mater.*, **44**, 1151–1154 (2008).
37. I. Pekgözlü, H. Karabulut, *Inorg. Mater.*, **45**, 61–64 (2009).
38. D. L. Dexter, J. H. Schulman, *J. Chem. Phys.*, **22**, 1063 (1954).
39. W. Zhang, P. Xie, C. Duan, K. Yan, M. Yin, L. Lou, S. Xia, J.-C. Krupa, *Chem. Phys. Lett.*, **292**, 133–136 (1998).
40. A. Manavbasi, J. C. LaCombe, *J. Lumin.*, **128**, 129–134 (2008).
41. S. F. Wang, M. K. Lü, F. Gu, C. F. Song, D. Xu, D. R. Yuan, G. J. Zhou, Y. X. Qi, *Inorg. Chem. Commun.*, **6**, 185–188 (2003).
42. Z. Xiu, S. Liu, F. Xu, M. Ren, J. Pan, X. Cui, W. Yu, J. Yu, *J. Alloys Compd.*, **441**, 219–221 (2007).
43. E. Erdoğan, İ. Pekgözlü, E. Korkmaz, A. S. Başak, *J. Appl. Spectrosc.*, **81**, 336–340 (2014).
44. L. Wu, Y. Zhang, Y. F. Kong, T. Q. Sun, J. J. Xu, X. L. Chen, *Inorg. Chem.*, **13**, 5207–5211 (2007).
45. G. Blasse, S. J. M. Sas, W. M. A. Smit, *Mater. Chem. Phys.*, **14**, 253–258 (1986).